Recovery of Hypoxic Regions in a Rat Model of Microembolism

Theodosia Georgakopoulou, M.Sc,[1] Anne-Eva van der Wijk, Ph.D,[1] Erik N.T.P. Bakker, Ph.D, and Ed vanBavel, Ph.D, on behalf of the INSIST investigators

Objectives: Endovascular treatment (EVT) has become the standard of care for acute ischemic stroke. Despite successful recanalization, a limited subset of patients benefits from the new treatment. Human MRI studies have shown that during removal of the thrombus, a shower of microclots is released from the initial thrombus, possibly causing new ischemic lesions. The aim of the current study is to quantify tissue damage following microembolism. *Materials and methods:* In a rat model, microembolism was generated by injection of a mixture of polystyrene fluorescent microspheres (15, 25 and 50 μm in diameter). The animals were killed at three time-points: day 1, 3 or 7. AMIRA and IMARIS software was used for 3D reconstruction of brain structure and damage, respectively. *Conclusions:* Microembolism induces ischemia, hypoxia and infarction. Infarcted areas persist, but hypoxic regions recover over time suggesting that repair processes in the brain rescue the regions at risk.

Key Words: Stroke—Microembolism—Ischemia—Hypoxia—Infarction

Introduction

Acute ischemic stroke accounts for about 80% of stroke cases.[1] The introduction of endovascular treatment (EVT), where a thrombus is removed by means of a retrieval device, has led to a breakthrough for the therapy of acute ischemic stroke.[2] However, although in the large majority of cases successful recanalization of the occluded vessel is attained[3,4], only one third of patients is left with a good clinical outcome, defined as modified Rankin Scale from 0 to 2 at 90 days follow-up.[5]

This discrepancy between successful recanalization and poor clinical outcome has been attributed to, among others, poor collateral status[6], hyperglycemia and site of occlusion.[4] Less attention is given to the release of emboli from the initial clot. There is evidence from human MRI studies that during and following removal of a thrombus, a shower of microclots releases from the initial thrombus and spreads in the arterial bed distal to the thrombus, possibly causing new ischemic lesions.[7,8] Based on in vitro simulations of EVT, hundreds of thousands of microemboli ranging in size from 10 μm to 1 mm were reported to be released into the cerebral circulation.[9] Although new generation devices generate less microthrombi[9], the number is still substantial and may be related to poor clinical outcome. While release of mm-size thrombi should clearly be avoided, less is known on the effect of small but very numerous micro-thrombi. Such effects are relevant for future device design.

Several studies have evaluated tissue damage and neurological deficits caused by microembolism. It was shown that the number of microemboli determines brain tissue damage and neurological deficit[10,11], and that the size of the particle determines the different injury patterns of cerebral infarction.[12,13] However, there is a lack of quantitative data regarding the course of brain damage in terms of ischemia, hypoxia and infarction as well as three-dimensional representations of tissue damage. This is needed to increase our understanding of stroke and improve EVT treatment.

The aim of the present study is to quantify tissue ischemia, hypoxia and infarction over time in a rat model of microembolism. We therefore injected a mixture of microspheres via the left common carotid artery and killed the animals at day (D) 1, 3 or 7. We hypothesize that

From the Amsterdam UMC, University of Amsterdam, Biomedical Engineering and Physics, Amsterdam Cardiovascular Sciences, Amsterdam, the Netherlands.

Received January 11, 2021; revision received March 1, 2021; accepted March 2, 2021.

Corresponding author. E-mail: e.vanbavel@amsterdamumc.nl.

[1]Both authors shared first authorship.

1052-3057/$ - see front matter

https://doi.org/10.1016/j.jstrokecerebrovasdis.2021.105739

microembolism relevant for EVT, ranging in size from 15−50 μm, is sufficient to cause brain damage. We found that microembolism induces ischemia, hypoxia and infarction, yet hypoxic regions became significantly less pronounced over time, indicating that the brain has the capacity to recover from hypoxic injury.

Methods

Microembolism surgery

Female and male Wistar rats (16 to 20 weeks old, Charles River) were used. Microembolism was generated by injecting a mixture of polystyrene fluorescent microspheres (25,000 of 15 μm, 5500 of 25 μm and 625 of 50 μm diameter). All experiments were performed under the approval of the local committee on the Ethics of Animal Experiments of the University of Amsterdam, University Medical Center (permit number: DMF321AA) and according to the ARRIVE guidelines and European Union guidelines for the care laboratory animals (Directive 2010/63/EU). The rats were housed in pairs in standard plastic cages with ad libitum food and water and a 12h:12h light-dark cycle. Microembolism surgeries were performed under anesthesia (isoflurane mixed with 100% O_2). Anesthesia was induced at 4% isoflurane (Isoflutek 1000 mg/g; Laboratorios Karizoo SA, Barcelona, Spain) in 1 L/min O_2, hair was removed from the neck caudal to the mandibles and buprenorphine (Temgesic™, 0.05 mg/kg, Schering-Plough, Welwyn Garden City, Hertfordshire, UK) was injected s.c. 30 min pre-surgery as analgesic. After placing the rat in a supine position on a heating pad, anesthesia was maintained (at 2-2.5% isoflurane in 1 L/min O_2) and body temperature was kept at 37.0±0.5 °C. Iodide was used to disinfect the skin and a ventral midline incision was made in the neck. The left common carotid artery, external carotid artery, and internal carotid artery were exposed. The external carotid artery and occipital artery were temporarily ligated with a 6.0 surgical suture. A mixture of fluorescent microspheres (DiagPoly™ Plain Fluorescent Polystyrene Particles, DFO-L011, DFO-L013, DFO-L016, λ Excitation 530 nm, λ Emission 582 nm, Creative Diagnostics®, Shirley, NY) was administered via the left common carotid artery using a 29 G insulin needle over a period of 30 s (15 ,25 and 50 μm microspheres, resuspended in a sterile 2% bovine serum albumin solution of phosphate buffered saline (PBS), in a total volume of 200 μl). The selected range of injected microspheres was based on the distribution of microemboli after in vitro EVT[9], but was limited only to sizes <50 μm to avoid whole brain infarct volumes. Microspheres ended up in the left hemisphere, leaving the contralateral side to serve as a control. Following removal of the needle, pressure was applied to the injection site to stop the bleeding. Finally, interrupted sutures (size 4−0) were made to close the wound and rats were allowed to recover on a heating pad before being placed back into their cages. Rats were randomly assigned to the three groups of D 1, 3 and 7.

Tissue preparation

Animals were killed on D1 (n=6; 3 female, 3 male), 3 (n=6; 2 female, 4 male) or 7 (n=7; 4 female, 3 male) post-surgery. For the detection of hypoxia, 60 mg/kg pimonidazole hydrochloride (Hypoxyprobe™ Pacific Blue Kit, HP15-x, Burlington, MA) was injected i.p. 90 min prior to euthanasia. To label the vasculature, DyLight 594 labeled tomato lectin (1 mg/kg; Vector Laboratories Cat# DL-1177) was administered via the tail vein and allowed to circulate for 5 min. Following injection of 100 μl heparin i.p. to avoid formation of blood clots, transcardial perfusion was done with heparinized PBS followed by tissue fixation with 4% paraformaldehyde at 80 mmHg. All aforementioned steps were performed while under anesthesia. Brains were then harvested for further processing.

Immunofluorescence staining

For immunofluorescent staining, brain sections (50 μm thick) were washed in PBS and incubated in blocking buffer (10% (v/v) normal goat serum (vector labs), 2 (v/v) TritonX-100 and 0.2% NaN3 in PBS) for 1 h at room temperature. Next, brain sections were incubated overnight at room temperature with primary antibody mouse anti-NeuN (1:200; Millipore Cat# MAB377). After washing, secondary antibodies goat anti-mouse Cy5 (1 1000; Thermo Fisher Scientific Cat# A10524) and mouse anti-pimonidazole (1:500; Hypoxyprobe™ Pacific Blue Kit, HP15-x) were added and brain sections were incubated for 2 h (for each antibody separately to avoid cross-reaction) at room temperature. All antibodies were incubated in blocking buffer. After washing, brain sections were sealed with fluorescence mounting medium (DAKO North America Inc., s3023). All staining procedures were performed under gentle agitation.

Confocal imaging and 3D analysis workflow

For each animal, ten consecutive coronal sections (50 μm thick) without cutting damage or major artefacts were selected within a distance between 1 and 5.5 mm from the bregma. The thickness of the sections and their distance from the bregma was chosen to facilitate 3D reconstruction.[14] Tilescan images of whole brain sections and z-stack tilescan images of the intervention hemisphere were acquired using a confocal laser scanning microscope SP8 (Leica Microsystems, Wetzlar, Germany) with a 10x objective. The z-stacks (5 μm steps) of each 50 μm section were then converted to maximum intensity projection images using Image J (Rasband, W.S., ImageJ, U. S. National Institutes of Health, Bethesda, Maryland, USA). This conversion was needed to facilitate the alignment of the sections, using AMIRA software (Visage Imaging, Inc., San Diego, CA, USA) as described by De Bakker et al, 2016.[15] Each aligned

maximum intensity projection section was inserted in IMARIS 9.3 software (Bitplane Inc., St. Paul, MN, USA) as an image of 50 μm thickness. As a result, a 500 μm thick brain volume was reconstructed per animal and further analyzed in IMARIS 9.3 software.

Lectin was injected intravenously to stain the endothelial luminal surface and the absence of lectin was used as a marker of ischemia. Pimonidazole hydrochloride (Hypoxyprobe™) binds to cells that have a partial oxygen pressure of ≤10 mmHg and was used as a marker of hypoxia. Anti-NeuN antibody binds to healthy neurons, and therefore absence of NeuN staining was used as a marker of infarction. For the hypoxic volume segmentation, the same batch of settings was applied to all brain volumes using the surface creation wizard of IMARIS 9.3. The ischemic and infarction volumes were segmented manually. The microspheres were automatically segmented using the spot creation wizard. Measurements of ischemic, hypoxic and infarcted volumes were performed in a randomized and blinded fashion regarding the day of sacrifice. The data are available from the corresponding author upon reasonable request.

Statistics

Normality of the data was tested by Shapiro-Wilk test. Normally distributed data are depicted as mean ± standard deviation and not normally distributed data as median and interquartile range. Differences between groups (D1, 3 and 7) were determined using analysis of variance followed by Tukey's test for multiple comparisons or Kruskal-Wallis followed by Dunn's test for multiple comparisons. Differences were considered statistically significant when $P \leq 0.05$. Statistical analyses and graphing were performed using GraphPad Prism 6 software (GraphPad Software, La Jolla, CA) and IMARIS 9.3.

Results

Microembolism causes ischemic, hypoxic and infarcted regions in the brain

Microembolism caused multiple focal lesions spread throughout the whole brain volume. Typical examples of individual coronal brain sections at different time-points are shown in Fig. 1A (white arrows indicate lesion locations). The lesions were characterized by ischemia (absence of lectin), hypoxia (hypoxyprobe) and infarction (absence of NeuN) (Supplementary Material Video 1) and were present at D1 (Fig. 1B top), D3 (Fig. 1B middle) and D7 (Fig. 1B bottom). In all cases, microspheres were confined to the intervention side, and no signs of tissue damage were found on the control side (Fig. 1B). In addition to the microscopic findings, macroscopic perivascular and point-like hemorrhages were regularly observed at all time-points when harvesting the brain (Supplementary Fig. 1).

Little but persistent neuronal damage 7 days following microembolism

To quantitatively assess tissue infarction, we reconstructed 500 μm thick brain volumes and quantified the

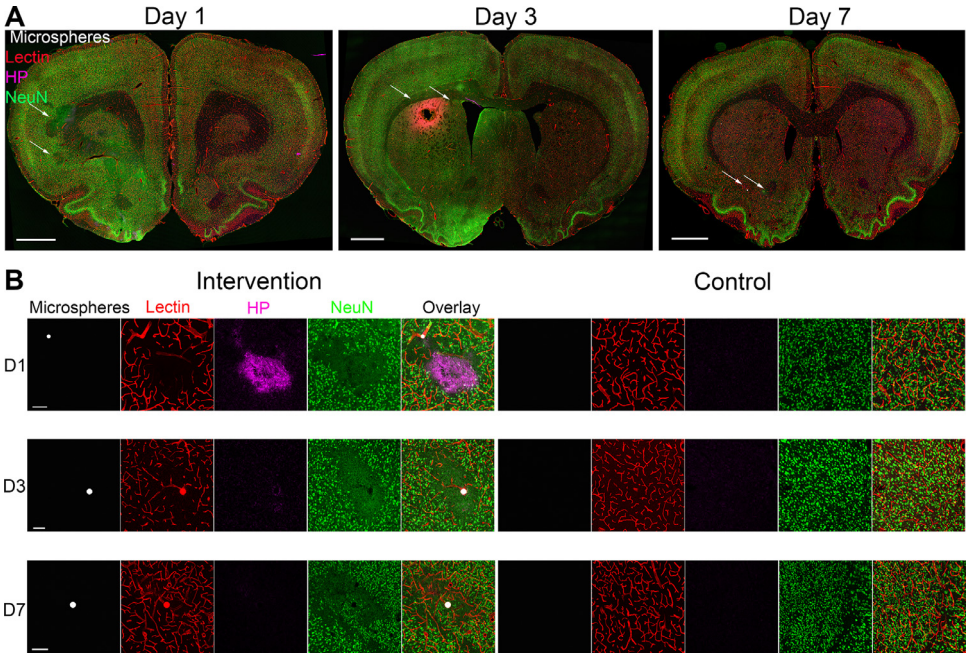

Fig. 1. *Multiple lesions following microembolism.* ***(A)*** *Multiple ischemic (absence of lectin; red), hypoxic (HP; hypoxyprobe; magenta) and infarcted regions (white arrows, absence of NeuN; green) in the intervention hemisphere as compared to the intact control hemisphere at D1, 3 and 7. Scale bar = 1500 μm.* ***(B)*** *Example of a microsphere (white) causing ischemia (absence of lectin; red), hypoxia (magenta) and infarction (absence of NeuN; green) at D1, causing ischemia, hypoxia and infarction at D3 and causing infarction at D7. Control side showed no signs of damage. Scale bar = 100 μm (For interpretation of the references to color in this figure legend, the reader is referred to the web version of this article.).*

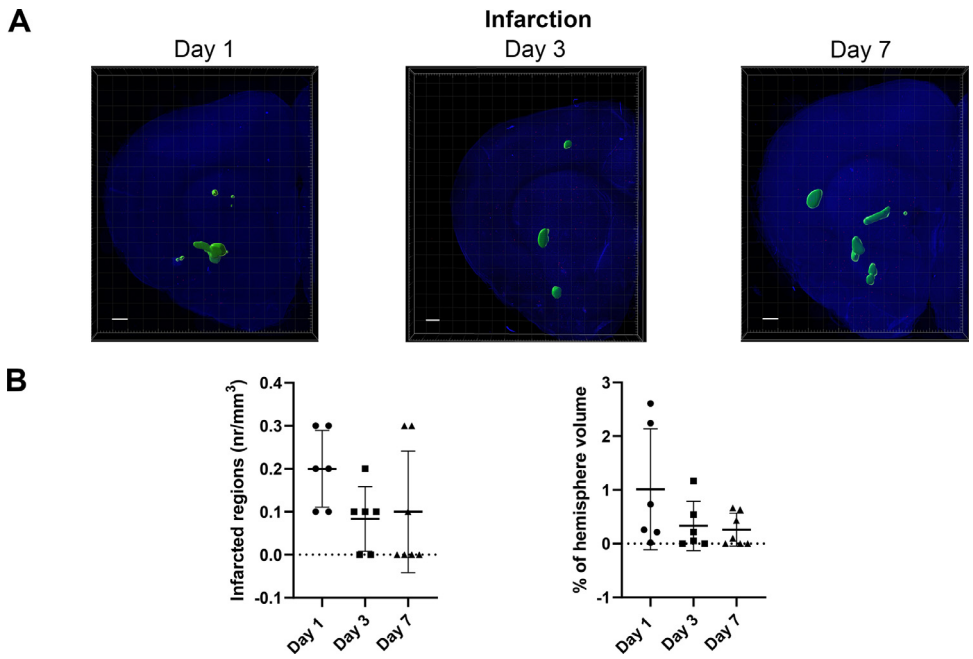

Fig. 2. *Infarcted areas persist over time.* ***(A)*** *Representative reconstructed brain volumes of the intervention hemisphere (blue) with segmented infarcted regions (green) and lodged microspheres (red) at D1, 3 and 7. Scale bar = 500 μm.* ***(B)*** *Quantification of the number of infarcted regions per mm^3 (left graph) and of the percentage of hemisphere being infarcted (right graph) at D1, 3 and 7. N = 6,7 animals per time-point. Data are depicted as mean ± standard deviation. Analysis of variance with Tukey's multiple comparison test (For interpretation of the references to color in this figure legend, the reader is referred to the web version of this article.).*

number and volumes of the infarcted regions (absence of NeuN). Tissue infarction was present at all three time-points (Fig. 2A). The number of infarcted regions as well as the total infarcted volume did not significantly change over time (Fig. 2B, left graph; P=0.1599, right graph; P=0.1492 not significant Analysis of variance). In brief, following microembolism a small fraction of the brain (<1%) became infarcted and this neuronal damage persisted.

Local cerebral ischemia and hypoxia recover within 7 days following microembolism

Next to infarction, we detected ischemic (absence of lectin) and hypoxic (hypoxyprobe) regions which were present at all three time-points (Fig. 3A,C; Supplementary Material Video 2). The number and total volume of ischemic and hypoxic regions significantly reduced over time (Fig. 3B, left graph; D1 vs D3: P=0.0548, D1 vs D7: P=0.0132, D3 vs D7: P>0.9999, right graph; D1 vs D3: P=0.1344, D1 vs D7: P=0.0245, D3 vs D7: P>0.9999, Dunn's multiple comparison test after significant Kruskal-Wallis and Fig. 3D, left graph; D1 vs D3: P=0.0071, D1 vs D7: P<0.0003, D3 vs D7: P=0.3443, right graph; D1 vs D3: P=0.0129, D1 vs D7: P<0.0026, D3 vs D7: P=0.7983, Tukey's multiple comparison test after significant analysis of variance). Notably, ischemia and hypoxia at D7 was virtually absent, suggesting successful reperfusion and recovery of hypoxic tissue at risk.

Discussion

To our knowledge, this is the first study to comprehensively map ischemia, hypoxia and infarction over time after cerebral microembolism. We found that microspheres of sizes relevant for EVT induced persistent neuronal damage, which did not change in terms of number and size over time. However, hypoxic and ischemic volumes had virtually disappeared after 7 days. These data suggest recovery of brain regions at risk within seven days.

In the majority of cases, EVT is preceded by thrombolysis with tissue plasminogen activator (rt-PA). However, the effectiveness of these agents is limited to the first 4.5 h after symptom onset[16], while also considerable time elapses during transport from local centers performing the thrombolysis to specialized centers for EVT. rt-PA would only be able to dissolve the microclots after recanalization of the major thrombus. As a result, a substantial number of microthrombi could remain in the microcirculation without being lysed. In mice injected with fibrin-rich microclots, almost half of the injected clots were found in the blood vessels even after administration of tissue plasminogen activator.[17]

This raises the question whether it would be sensible to perform thrombolysis also *after* the EVT. To our knowledge, no randomized clinical trials included rt-PA administration after EVT[18,19], as can be appreciated because of the high risk of symptomatic intracranial hemorrhage[20], a common complication of the drug. The only data on the use of thrombolytic treatment after EVT come from case reports of patients

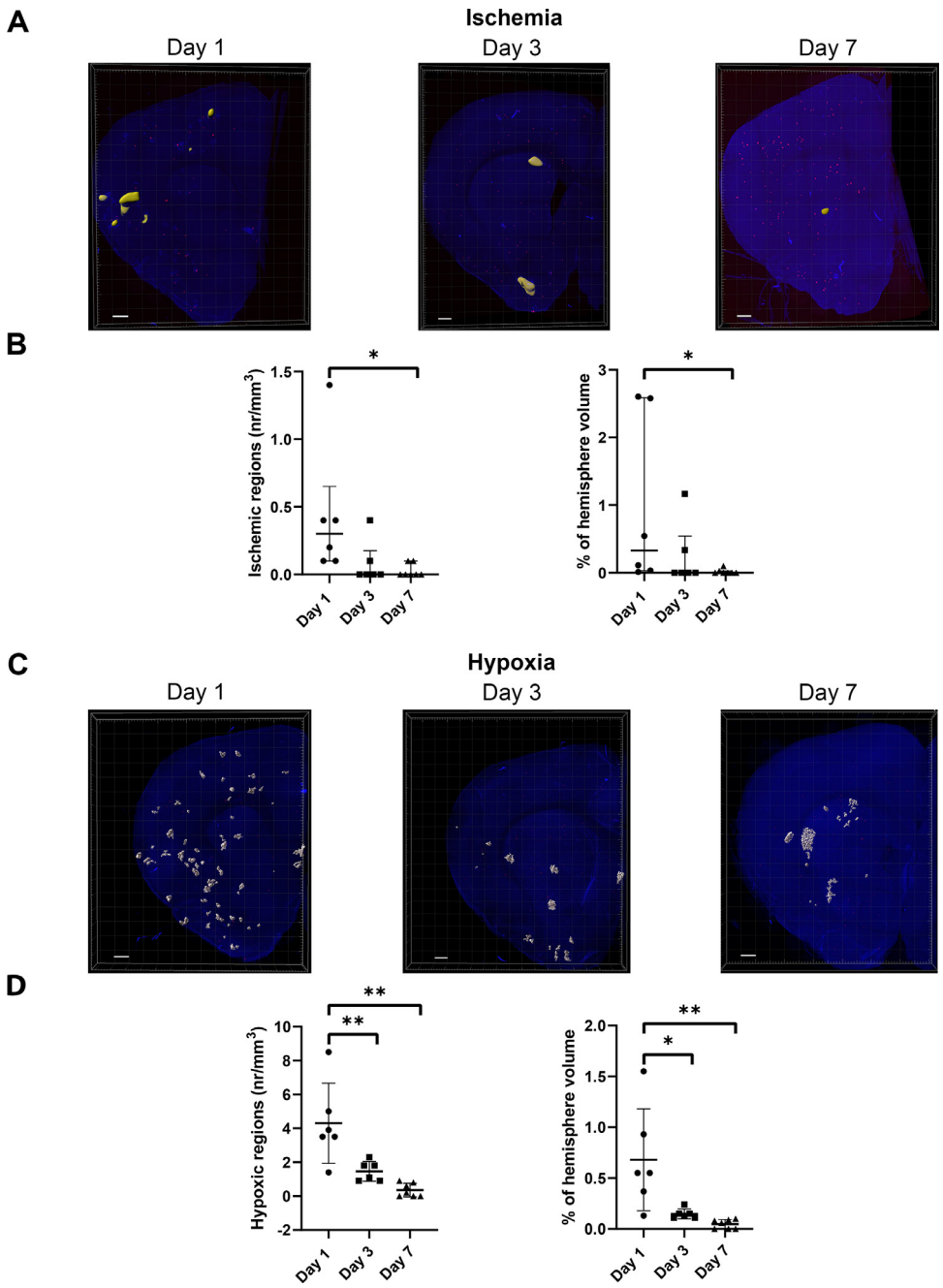

Fig. 3. *Ischemia and hypoxia decline over time* ***(A)*** *Representative reconstructed brain volumes of the intervention hemisphere (blue) with segmented ischemic regions (yellow) and lodged microspheres (red) at D1, 3 and 7. Scale bar = 500 μm.* ***(B)*** *Quantification of the number of ischemic regions per mm^3 (left graph) and of the percentage of hemisphere being ischemic (right graph) at D1, 3 and 7.* N = *6,7 animals per time-point. Data are depicted as median and interquartile range.* *P*<0.05, D1 vs D7, Kruskal-Wallis with Dunn's multiple comparisons test.* ***(C)*** *Representative reconstructed brain volumes of the intervention hemisphere (blue) with segmented hypoxic regions (grey) and lodged microspheres (red) at D1, 3 and 7. Scale bar = 500 μm.* ***(D)*** *Quantification of the number of hypoxic regions per mm^3 (left graph) and of the percentage of hemisphere being hypoxic (right graph) at D1, 3 and 7.* N = *6,7 animals per time-point. Data are depicted as mean ± standard deviation.* **P*<0.01, *P*<0.05, D1 vs D3 and D1 vs D7. Analysis of variance with Tukey's multiple comparison test (For interpretation of the references to color in this figure legend, the reader is referred to the web version of this article.).*

with recurrent stroke within 90 days from their prior event.[21,22] Despite the contraindication of using rt-PA in this subset of patients, a small systematic review[23] concluded that repeated rt-PA administration may not be as harmful as initially thought. Due to the limited data it is hard to determine whether such treatment will be beneficial for patients. In addition, clots are very heterogeneous and can be rich in fibrin, but also in red blood cells, white blood cells and platelets[24] which may impair their susceptibility to thrombolysis.[25] Moreover, since microthrombi cannot be visualized with the current clinical imaging modalities, their fate

after such adjunctive therapy would remain unknown, and only functional outcome could be assessed. Following successful thrombus removal, rt-PA might have a higher likelihood of reaching the distal microthrombi, but there seem few arguments for performing clinical trials on this prior to more extensive translational research.

Next to thrombolysis, angiophagy is a complementary mechanism of the brain for vascular recanalization, where the embolus is enveloped by endothelial membrane projections and subsequently extravasated to the brain parenchyma.[26,27] In the present study, the reduction in number and size of ischemic volumes over time indicates successful local reperfusion. The mechanisms of local flow recovery were addressed in another study from our group, where we showed that at D7 almost half of the lodged microspheres are extravasated.[28] Based on these findings, the successful local reperfusion found in the current study may relate to angiophagy.

The microembolism model we developed can be used to quantify transient and persistent effects of microemboli on the brain tissue, following EVT. The selection of microspheres instead of fibrin clots was made for two reasons. Firstly, microspheres are not biodegradable and not susceptible to thrombolysis, covering a broad spectrum of persistent occluding materials. Secondly, the size, shape and number of microspheres can be controlled, making it possible to occlude the desired vascular level.

A limitation of this study is that we did not test the effect of individual sizes of microspheres. Lam *et al.* observed transient hypoxia but no infarctions for 10 or 15 μm microspheres in mice.[26] It remains to be established whether the current infarctions are caused by the combination of different sizes or rather just the 25 and 50 μm microspheres. Also, future work needs to address the spatial relationship between embolus and brain damage, as well as the cooperative effects of multiple microspheres of varying size.

Here, we did not combine microembolism with a large vessel occlusion. We intentionally chose this approach in order to isolate the local consequences of microemboli. We expect that the local effects due to obstructed arterioles and capillaries will be analogous for rat and human, since the capillaries have the same diameter and arteriolar density is comparable for these species.[29,30] For the same reason we selected this particular range of microsphere sizes between 15 and 50 μm, although the emboli released after in vitro EVT also include larger sizes.[9] It remains to be established how representative these data are for penumbral and healthy areas in stroke. A rat study found that unilateral proximal carotid occlusion is insufficient to cause stroke but strongly increases lesion sizes caused by 50 micron microspheres[31], suggesting mutual influence of local and global occlusions on cerebral injury.

In conclusion, our study demonstrated that microspheres with sizes resembling microthrombi in EVT induce irreversible micro-infarcts as well as areas of ischemia and hypoxia that recover within 7 days. These effects are relevant in major strokes for tissue damage progression, in areas of the target downstream territory with normal macroscopic perfusion, or in the penumbra.

Author contributions

ENTPB, EvB, AEvdW and TG designed the experiments; TG and AEvdW performed the surgeries; TG analyzed the data and wrote the manuscript; AEvdW, ENTPB and EvB contributed to editing of the manuscript. All authors read and approved the final version of the manuscript.

Funding

This project was funded from the European Union's Horizon 2020 research and innovation program under grant agreement No. 777072 (INSIST).

Declaration of Competing Interest

The authors declare that the research was conducted in the absence of any commercial or financial relationships that could be construed as a potential conflict of interest.

Acknowledgments

We thank Jaco Hagoort of the Medical Biology Department (Amsterdam UMC) and Marjolijn Mertz of the Netherlands Cancer Institute for assisting with AMIRA and IMARIS respectively.

Supplementary materials

Supplementary material associated with this article can be found in the online version at doi:10.1016/j.jstrokecerebrovasdis.2021.105739.

References

1. Bamford J, Sandercock P, Dennis M, et al. Classification and natural history of clinically identifiable subtypes of cerebral infarction. Lancet 1991;337:1521-1526.
2. Berkhemer OA, Fransen PS, Beumer D, et al. A randomized trial of intraarterial treatment for acute ischemic stroke. N Engl J Med 2015;372:11-20.
3. Nogueira RG, Lutsep HL, Gupta R, et al. Trevo versus merci retrievers for thrombectomy revascularisation of large vessel occlusions in acute ischaemic stroke (TREVO 2): a randomised trial. Lancet 2012;380:1231-1240.
4. Bhaskar S, Stanwell P, Cordato D, et al. Reperfusion therapy in acute ischemic stroke: dawn of a new era? BMC Neurol 2018;18:8.
5. Munich SA, Vakharia K, Levy EI. Overview of mechanical thrombectomy techniques. Neurosurgery 2019;85. S60-s67.
6. Berkhemer OA, Jansen IG, Beumer D, et al. Collateral status on baseline computed tomographic angiography and intra-arterial treatment effect in patients with proximal anterior circulation stroke. Stroke 2016;47:768-776.

7. Palombo G, Faraglia V, Stella N, et al. Late evaluation of silent cerebral ischemia detected by diffusion-weighted MR imaging after filter-protected carotid artery stenting. AJNR Am j Neuroradiol 2008;29:1340-1343.
8. Zhu L, Wintermark M, Saloner D, et al. The distribution and size of ischemic lesions after carotid artery angioplasty and stenting: evidence for microembolization to terminal arteries. J Vasc Surg 2011;53:971-975. discussion 975-976.
9. Chueh JY, Kuhn AL, Puri AS, et al. Reduction in distal emboli with proximal flow control during mechanical thrombectomy: a quantitative in vitro study. Stroke 2013;44:1396-1401.
10. Atochin DN, Murciano JC, Gursoy-Ozdemir Y, et al. Mouse model of microembolic stroke and reperfusion. Stroke 2004;35:2177-2182.
11. Winding O. Cerebral microembolization following carotid injection of dextran microspheres in rabbits. Neuroradiology 1981;21:123-126.
12. Tsai MJ, Tsai YH, Kuo YM. Characterization of the pattern of ischemic stroke induced by artificial particle embolization in the rat brain. Biomaterials 2011;32:6381-6388.
13. Rapp JH, Pan XM, Yu B, et al. Cerebral ischemia and infarction from atheroemboli <100 μm in size. Stroke 2003;34:1976-1980.
14. Luzzati F, Fasolo A, Peretto P. Combining confocal laser scanning microscopy with serial section reconstruction in the study of adult neurogenesis. Front Neurosci 2011;5:70.
15. de Bakker BS, de Jong KH, Hagoort J, et al. An interactive three-dimensional digital atlas and quantitative database of human development. Science 2016:354.
16. Wardlaw JM, Murray V, Berge E, et al. Recombinant tissue plasminogen activator for acute ischaemic stroke: an updated systematic review and meta-analysis. Lancet 2012;379:2364-2372.
17. Grutzendler J, Murikinati S, Hiner B, et al. Angiophagy prevents early embolus washout but recanalizes microvessels through embolus extravasation. Sci Transl med 2014;6. 226ra231.
18. Saver JL, Adeoye O. Intravenous thrombolysis before endovascular thrombectomy for acute ischemic stroke. JAMA 2021;325:229-231.
19. Phipps MS, Cronin CA. Management of acute ischemic stroke. BMJ 2020;368:l6983.
20. Tsivgoulis G, Kargiotis O, Alexandrov AV. Intravenous thrombolysis for acute ischemic stroke: a bridge between two centuries. Expert Rev Neurother 2017;17:819-837.
21. Alhazzaa M, Sharma M, Blacquiere D, et al. Thrombolysis despite recent stroke: a case series. Stroke 2013;44:1736-1738.
22. Yoo HS, Kim YD, Lee HS, et al. Repeated Thrombolytic Therapy in patients with recurrent acute ischemic stroke. J Stroke 2013;15:182-188.
23. Sarmiento RJC, Diestro JDB, Espiritu AI, et al. Safety and efficacy of repeated thrombolysis with alteplase in early recurrent ischemic stroke: a systematic review. J Stroke Cerebrovasc Dis 2019;28:104290.
24. Fitzgerald S, Dai D, Wang S, et al. Platelet-rich emboli in cerebral large vessel occlusion are associated with a large artery atherosclerosis source. Stroke 2019;50:1907-1910.
25. Wohner N, Sótonyi P, Machovich R, et al. Lytic resistance of fibrin containing red blood cells. Arterioscler Thromb Vasc Biol 2011;31:2306-2313.
26. Lam CK, Yoo T, Hiner B, et al. Embolus extravasation is an alternative mechanism for cerebral microvascular recanalization. Nature 2010;465:478-482.
27. van der Wijk AE, Lachkar N, de Vos J, et al. Extravasation of microspheres in a rat model of silent brain infarcts. Stroke 2019;50:1590-1594.
28. van der Wijk A-E, Georgakopoulou T, Majolée J, et al. Microembolus clearance through angiophagy is an auxiliary mechanism preserving tissue perfusion in the rat brain. Acta Neuropathol Commun 2020;8:195.
29. Reina-De La Torre F, Rodriguez-Baeza A, Sahuquillo-Barris J. Morphological characteristics and distribution pattern of the arterial vessels in human cerebral cortex: a scanning electron microscope study. Anat Rec 1998;251:87-96.
30. Ngai AC, Winn HR. Modulation of cerebral arteriolar diameter by intraluminal flow and pressure. Circ Res 1995;77:832-840.
31. Omae T, Mayzel-Oreg O, Li F, et al. Inapparent hemodynamic insufficiency exacerbates ischemic damage in a rat microembolic stroke model. Stroke 2000;31:2494-2499.